A Path Independent Integral and the Approximate Analysis of Strain Concentration by Notches and Cracks

J. R. RICE
Assistant Professor of Engineering,
Brown University,
Providence, R. I.

A line integral is exhibited which has the same value for all paths surrounding the tip of a notch in the two-dimensional strain field of an elastic or deformation-type elastic-plastic material. Appropriate integration path choices serve both to relate the integral to the near tip deformations and, in many cases, to permit its direct evaluation. This averaged measure of the near tip field leads to approximate solutions for several strain-concentration problems. Contained perfectly plastic deformation near a crack tip is analyzed for the plane-strain case with the aid of the slip-line theory. Near tip stresses are shown to be significantly elevated by hydrostatic tension, and a strain singularity results varying inversely with distance from the tip in centered fan regions above and below the tip. Approximate estimates are given for the strain intensity, plastic zone size, and crack tip opening displacement, and the important role of large geometry changes in crack blunting is noted. Another application leads to a general solution for crack tip separations in the Barenblatt-Dugdale crack model. A proof follows on the equivalence of the Griffith energy balance and cohesive force theories of elastic brittle fracture, and hardening behavior is included in a model for plane-stress yielding. A final application leads to approximate estimates of strain concentrations at smooth-ended notch tips in elastic and elastic-plastic materials.

Introduction

CONSIDERABLE mathematical difficulties accompany the determination of concentrated strain fields near notches and cracks, especially in nonlinear materials. An approximate analysis of a variety of strain-concentration problems is carried out here through a method which bypasses this detailed solution of boundary-value problems. The approach is first to identify a line integral which has the same value for all integration paths surrounding a class of notch tips in two-dimensional deformation fields of linear or nonlinear elastic materials. The choice of a near tip path directly relates the integral to the locally concentrated strain field. But alternate choices for the path often permit a direct evaluation of the integral. This knowledge of an averaged value for the locally concentrated strain field is the starting point in the analysis of several notch and crack problems discussed in subsequent sections.

All results are either approximate or exact in limiting cases. The approximations suffer from a lack of means for estimating errors or two-sided bounds, although lower bounds on strain magnitudes may sometimes be established. The primary interest in discussing nonlinear materials lies with elastic-plastic behavior in metals, particularly in relation to fracture. This behavior is best modeled through incremental stress-strain relations. But no success has been met in formulating a path integral for incremental plasticity analogous to that presented here for elastic materials. Thus a "deformation" plasticity theory is employed and the phrase "elastic-plastic material" when used here will be understood as denoting a nonlinear elastic material exhibiting a linear Hookean response for stress states within a yield surface and a nonlinear hardening response for those outside.

Contributed by the Applied Mechanics Division and presented at the Applied Mechanics Conference, Providence, R. I., June 12–14, 1968, of THE AMERICAN SOCIETY OF MECHANICAL ENGINEERS.

Discussion of this paper should be addressed to the Editorial Department, ASME, United Engineering Center, 345 East 47th Street, New York, N. Y. 10017, and will be accepted until July 15, 1968. Discussion received after the closing date will be returned. Manuscript received by ASME Applied Mechanics Division, May 22, 1967; final draft, March 5, 1968. Paper No. 68—APM-31.

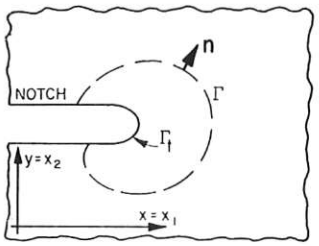

Fig. 1 Flat surfaced notch in two-dimensional deformation field (all stresses depend only on x and y). Γ is any curve surrounding the notch tip; Γ_t denotes the curved notch tip.

Path Independent J Integral. Consider a homogeneous body of linear or nonlinear elastic material free of body forces and subjected to a two-dimensional deformation field (plane strain, generalized plane stress, antiplane strain) so that all stresses σ_{ij} depend only on two Cartesian coordinates $x_1(= x)$ and $x_2(= y)$. Suppose the body contains a notch of the type shown in Fig. 1, having flat surfaces parallel to the x-axis and a rounded tip denoted by the arc Γ_t. A straight crack is a limiting case. Define the strain-energy density W by

$$W = W(x, y) = W(\boldsymbol{\varepsilon}) = \int_0^{\boldsymbol{\epsilon}} \sigma_{ij} d\epsilon_{ij}, \tag{1}$$

where $\boldsymbol{\varepsilon} = [\epsilon_{ij}]$ is the infinitesimal strain tensor. Now consider the integral J defined by

$$J = \int_\Gamma \left(W dy - \mathbf{T} \cdot \frac{\partial \mathbf{u}}{\partial x}\, ds \right). \tag{2}$$

Here Γ is a curve surrounding the notch tip, the integral being evaluated in a contraclockwise sense starting from the lower flat notch surface and continuing along the path Γ to the upper flat surface. $\mathbf{T}$ is the traction vector defined according to the outward normal along Γ, $T_i = \sigma_{ij} n_j$, $\mathbf{u}$ is the displacement vector, and ds is an element of arc length along Γ. To prove path independent, consider any closed curve Γ^* enclosing an area A^* in a

two-dimensional deformation field free of body forces. An application of Green's theorem [1][1] gives

$$\int_{\Gamma^*}\left(W dy - T_i \frac{\partial u_i}{\partial x} ds\right) = \int_{A^*}\left[\frac{\partial W}{\partial x} - \frac{\partial}{\partial x_j}\left(\sigma_{ij}\frac{\partial u_i}{\partial x}\right)\right] dx dy. \quad (3a)$$

Differentiating the strain-energy density,

$$\frac{\partial W}{\partial x} = \frac{\partial W}{\partial \epsilon_{ij}}\cdot\frac{\partial \epsilon_{ij}}{\partial x} = \sigma_{ij}\frac{\partial \epsilon_{ij}}{\partial x} \qquad \text{[by equation (1)]}$$

$$= \frac{1}{2}\sigma_{ij}\left[\frac{\partial}{\partial x}\left(\frac{\partial u_i}{\partial x_j}\right) + \frac{\partial}{\partial x}\left(\frac{\partial u_j}{\partial x_i}\right)\right]$$

$$= \sigma_{ij}\frac{\partial}{\partial x_j}\left(\frac{\partial u_i}{\partial x}\right) \qquad (\text{since } \sigma_{ij} = \sigma_{ji})$$

$$= \frac{\partial}{\partial x_j}\left(\sigma_{ij}\frac{\partial u_i}{\partial x}\right) \qquad \left(\text{since } \frac{\partial \sigma_{ij}}{\partial x_j} = 0\right) \quad (3b)$$

The area integral in equation (3a) vanishes identically, and thus

$$\int_{\Gamma^*}\left(W dy - \mathbf{T}\cdot\frac{\partial \mathbf{u}}{\partial x} ds\right) = 0 \qquad \text{for any closed curve } \Gamma^*. \quad (3c)$$

Consider any two paths Γ_1 and Γ_2 surrounding the notch tip, as does Γ in Fig. 1. Traverse Γ_1 in the contraclockwise sense, continue along the upper flat notch surface to where Γ_2 intersects the notch, traverse Γ_2 in the clockwise sense, and then continue along the lower flat notch surface to the starting point where Γ_1 intersects the notch. This describes a closed contour so that the integral of $W dy - \mathbf{T}\cdot(\partial \mathbf{u}/\partial x) ds$ vanishes. But $\mathbf{T} = 0$ and $dy = 0$ on the portions of path along the flat notch surfaces. Thus the integral along Γ_1 contraclockwise and the integral along Γ_2 clockwise sum to zero. J has the same value when computed by integrating along either Γ_1 or Γ_2, and path independent is proven. We assume, of course, that the area between curves Γ_1 and Γ_2 is free of singularities.

Clearly, by taking Γ close to the notch tip we can make the integral depend only on the local field. In particular, the path may be shrunk to the tip Γ_t (Fig. 1) of a smooth-ended notch and since $\mathbf{T} = 0$ there,

$$J = \int_{\Gamma_t} W dy \quad (4)$$

so that J is an averaged measure of the strain on the notch tip. The limit is not meaningful for a sharp crack. Nevertheless, since an arbitrarily small curve Γ may then be chosen surrounding the tip, the integral may be made to depend only on the crack tip singularity in the deformation field. The utility of the method rests in the fact that alternate choices of integration paths often permit a direct evaluation of J. These are discussed in the next section, along with an energy-rate interpretation of the integral generalizing work by Irwin [2] for linear behavior. The J integral is identical in form to a static component of the "energy-momentum tensor" introduced by Eshelby [3] to characterize generalized forces on dislocations and point defects in elastic fields.

Evaluation of the J Integral

Two Special Configurations. The J integral may be evaluated almost by inspection for the configurations shown in Fig. 2. These are not of great practical interest, but are useful in illustrating the relation to potential energy rates. In Fig. 2(a), a semi-infinite flat-surfaced notch in an infinite strip of height h, loads are applied by clamping the upper and lower surfaces of the strip so that the displacement vector $\mathbf{u}$ is constant on each clamped boundary. Take Γ to be the dashed curve shown which stretches out to $x = \pm\infty$. There is no contribution to J from the portion of Γ along the clamped boundaries since $dy = 0$ and $\partial \mathbf{u}/\partial x = 0$ there. Also at $x = -\infty$, $W = 0$ and $\partial \mathbf{u}/\partial x = 0$. The entire contribution to J comes from the portion of Γ at $x = +\infty$, and since $\partial \mathbf{u}/\partial x = 0$ there,

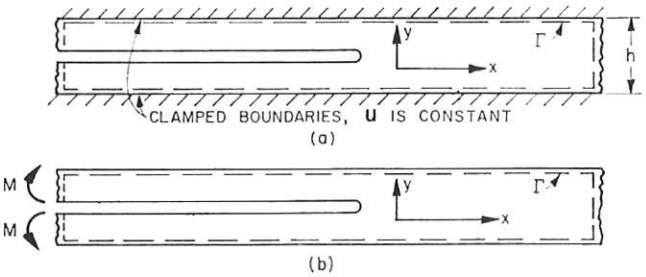

Fig. 2 Two special configurations for which the path independent integral J is readily evaluated on the dashed-line paths Γ shown. Infinite strips with semi-infinite notches. (a) Constant displacements imposed by clamping boundaries, and (b) pure bending of beamlike arms.

$$J = W_\infty h \quad (5)$$

where W_∞ is the constant strain-energy density at $x = +\infty$.

Now consider the similar configuration in Fig. 2(b), with loads applied by couples M per unit thickness on the beamlike arms so a state of pure bending (all stresses vanishing except σ_{xx}) results at $x = -\infty$. For the contour Γ shown by the dashed line, no contribution to J occurs at $x = +\infty$ as W and $\mathbf{T}$ vanish there, and no contribution occurs for portions of Γ along the upper and lower surfaces of the strip as dy and $\mathbf{T}$ vanish. Thus J is given by the integral across the beam arms at $x = -\infty$ and on this portion of Γ, $dy = -ds$, $T_y = 0$, and $T_x = -\sigma_{xx}$. We end up integrating

$$\sigma_{xx}\frac{\partial u_x}{\partial x} - W = \sigma_{xx}\epsilon_{xx} - W = \sigma_{ij}\epsilon_{ij} - W = \int_0^\sigma \epsilon_{ij} d\sigma_{ij} = \Omega \quad (6a)$$

across the two beam arms, where Ω is the complementary energy density. Thus, letting $\Omega_b(M)$ be the complementary energy per unit length of beam arm per unit thickness for a state of pure bending under moment per unit thickness M,

$$J = 2\Omega_b(M). \quad (6b)$$

Small Scale Yielding in Elastic-Plastic Materials. Consider a narrow notch or crack in a body loaded so as to induce a yielded zone near the tip that is small in size compared to geometric dimensions such as notch length, unnotched specimen width, and so on. The situation envisioned has been termed "small-scale yielding," and a boundary-layer style formulation of the problem [4] is profitably employed to discuss the limiting case. The essential ideas are illustrated with reference to Fig. 3. Loadings symmetrical about the narrow notch are imagined to induce a deformation state of plane strain. First, consider the linear elastic solution of the problem when the notch is presumed to be a sharp crack. Employing polar coordinates r, θ with origin at the crack tip, the form of stresses in the vicinity of the tip are known [2, 5] to exhibit a characteristic inverse square-root dependence on r:

$$\sigma_{ij} = \frac{K_I}{(2\pi r)^{1/2}} f_{ij}(\theta) + \text{other terms which are bounded at the crack tip.} \quad (7a)$$

Here K_I is the stress intensity factor and the set of functions $f_{ij}(\theta)$ are the same for all symmetrically loaded crack problems. For an isotropic material

[1] Numbers in brackets designate References at end of paper.

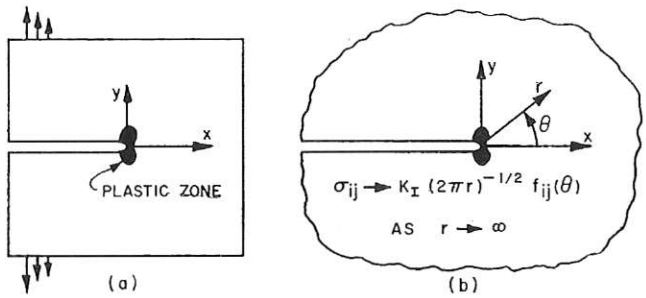

Fig. 3 *(a)* **Small-scale yielding near a narrow notch or crack in an elastic-plastic material.** *(b)* **The actual configuration is replaced by a semi-infinite notch or crack in an infinite body; actual boundary conditions are replaced by the requirement of an asymptotic approach to the linear elastic crack tip singularity stress field.**

$$f_{xx}(\theta) = \cos(\theta/2)[1 - \sin(\theta/2)\sin(3\theta/2)]$$
$$f_{yy}(\theta) = \cos(\theta/2)[1 + \sin(\theta/2)\sin(3\theta/2)] \qquad (7b)$$
$$f_{xy}(\theta) = f_{yx}(\theta) = \sin(\theta/2)\cos(\theta/2)\cos(3\theta/2).$$

Now suppose the material is elastic-plastic and the load level is sufficiently small so that a yield zone forms near the tip which is small compared to notch length and similar characteristic dimensions (small-scale yielding, Fig. 3(*a*)). One anticipates that the elastic singularity governs stresses at distances from the notch root that are large compared to yield zone and root radius dimensions but still small compared to characteristic geometric dimensions such as notch length. The actual configuration in Fig. 3(*a*) is then replaced by the simpler semi-infinite notch in an infinite body, Fig. 3(*b*), and a boundary-layer approach is employed replacing actual boundary conditions in Fig. 3(*a*) with the asymptotic boundary conditions

$$\sigma_{ij} \to \frac{K_I}{(2\pi r)^{1/2}} f_{ij}(\theta) \qquad \text{as } r \to \infty, \qquad (7c)$$

where K_I is the stress intensity factor from the linear elastic crack solution.

Such boundary-layer solutions for cracks are mathematically exact in the plastic region only to the first nonvanishing term of a Taylor expansion of complete solutions in the applied load. But comparison [4] with available complete solutions indicates the boundary-layer approach to be a highly accurate approximation up to substantial fractions (typically, one half) of net section yielding load levels. We now evaluate the integral J from the boundary-layer solution, taking Γ to be a large circle of radius r in Fig. 3(*b*):

$$J = r\int_{-\pi}^{+\pi}\left[[W(r,\theta)\cos\theta - \mathbf{T}(r,\theta)\cdot\frac{\partial \mathbf{u}}{\partial x}(r,\theta)\right]d\theta. \qquad (8a)$$

By path independence we may let $r \to \infty$ and since W is quadratic in strain in the elastic region, only the asymptotically approached inverse square-root elastic-stress field contributes. Working out the associated plane-strain deformation field, one finds

$$J = \frac{1-\nu^2}{E}K_I^2 \qquad \text{for small scale yielding,} \qquad (8b)$$

where E is Young's modulus and ν Poisson's ratio.

Primarily, we will later deal with one configuration, the narrow notch or crack of length $2a$ in a remotely uniform stress field σ_∞, Fig. 4. Here [2]

$$K_I = \sigma_\infty(\pi a)^{1/2}$$

and

$$J = \frac{\pi(1-\nu^2)}{E}\sigma_\infty^2 a \qquad \text{for small-scale yielding} \qquad (9)$$

For plane stress, the same result holds for J with $1 - \nu^2$ replaced by unity. The same computation may be carried out for more general loadings. Letting K_I, K_{II}, and K_{III} be elastic stress-intensity factors [2] for the opening, in-plane sliding, and antiplane sliding modes, respectively, of notch tip deformation one readily obtains

$$J = \frac{1-\nu^2}{E}(K_I^2 + K_{II}^2) + \frac{1+\nu}{E}K_{III}^2$$

(small-scale yielding) (10)

Interpretation in Terms of Energy Comparisons for Notches of Neighboring Size. Let A' denote the cross section and Γ' the bounding curve of a two-dimensional elastic body. The potential energy per unit thickness is defined as

$$P = \int_{A'} W dx dy - \int_{\Gamma''} \mathbf{T}\cdot\mathbf{u}\, ds, \qquad (11)$$

where Γ'' is that portion of Γ' on which tractions $\mathbf{T}$ are prescribed. Let $P(l)$ denote the potential energy of such a body containing a flat-surfaced notch as in Fig. 1 with tip at $x = l$. We compare this with the energy $P(l + \Delta l)$ of an identically loaded body which is similar in every respect except that the notch is now at $x = l + \Delta l$, the shape of the curved tip Γ_t being the same in both cases. Then one may show that

$$J = -\lim_{\Delta l \to 0}\frac{P(l+\Delta l) - P(l)}{\Delta l} = -\frac{\partial P}{\partial l}, \qquad (12)$$

the rate of decrease of potential energy with respect to notch size. The proof is lengthy and thus deferred for brevity to a section of a forthcoming treatise chapter [6]. Equations just mentioned provide a check. For loading by imposed displacements only as in Fig. 2(*a*), the potential energy equals the strain energy so that equation (5) results. Similarly, the potential energy equals minus the complementary energy for loading by tractions only as in Fig. 2(*b*), so that equation (6*b*) results. Equation (10) is the linear elastic energy-release rate given by Irwin [2], and reflects the fact that a small nonlinear zone at a notch tip negligibly affects the overall compliance of a notched body.

In view of the energy-rate interpretation of J and its alternate relation to the near tip deformation field, the present work provides a generalization of the connection between crack-tip stress-intensity factors and energy rates noted by Irwin for linear materials. Further, J. W. Hutchinson has noted in a private communication that an energy-rate line integral proposed by Sanders [7] for linear elasticity may be rearranged so as to coincide with the J integral form. The connection between energy rates and locally concentrated strains on a smooth-ended notch tip, as in equations (4) and (12), has been noted first by Thomas [8] and later by Rice and Drucker [9] and Bowie and Neal [10]. Since subsequent results on strain concentrations will be given in terms of J, means for its determination in cases other than those represented by equations (5)–(10) are useful. The energy-rate interpretation is pertinent here. In particular, the compliance testing method of elastic fracture mechanics [2] is directly extendable through equation (12) to nonlinear materials. Also, highly approximate analyses may be employed since only overall compliance changes enter the determination of J. For example, the Dugdale model

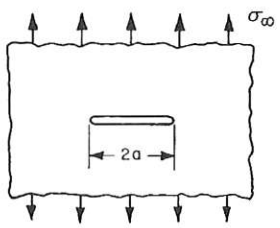

Fig. 4 Narrow notch or crack of length $2a$ in infinite body; uniform remote stress σ_∞

discussed next or simple antiplane strain calculations [11] may be employed to estimate the deviation of J from its linear elastic value in problems dealing with large-scale plastic yielding near a notch. Once having determined J (approximately), the model may be ignored and methods of the next sections employed to discuss local strain concentrations. Such estimates of J are given in reference [6] for the two models just noted. As anticipated, deviations from the linear elastic value show little sensitivity to the particular model employed.

Perfectly Plastic Plane-Strain Yielding at a Crack Tip

As a first application we consider the plane-strain problem of contained plastic deformation near a crack tip in a nonhardening material. Behavior is idealized as linear elastic until the principal in-plane shear stress reaches a yield value τ_Y, at which unrestricted further deformation may occur with no increase in shear stress. This conveniently permits utilization of the slip-line theory [12] in plastic regions. The idealization is rigorously correct for an isotropic nonhardening material exhibiting elastic as well as plastic incompressibility. Elastically compressible materials approach a constant in-plane shear stress in plastic regions when plastic strains are somewhat in excess of initial yield values, as anticipated in the near crack tip region. Constancy of the J integral requires a displacement gradient singularity at the crack tip since stresses are bounded and the path may be shrunk to zero length. Thus we construct a near tip stress state satisfying the yield condition and varying only with the polar angle θ.

The slip lines of this field are shown in Fig. 5. Traction-free boundary conditions require yield in uniaxial tension along the crack line and the 45-deg slip lines carry this stress state into the isosceles right triangle A:

$$\sigma_{xx} = 2\tau_Y, \qquad \sigma_{yy} = \sigma_{xy} = 0 \qquad \text{(region A)} \qquad (13a)$$

Any slip line of region A finding its way to the x-axis in front of the crack must swing through an angle of $\pi/2$. The accompanying hydrostatic stress elevation [12] and 45-deg slip lines determine the constant stress state

$$\sigma_{xx} = \pi\tau_Y, \qquad \sigma_{yy} = (2 + \pi)\tau_Y,$$
$$\sigma_{xy} = 0 \qquad \text{(region B)} \qquad (13b)$$

in the diamond-shaped region ahead of the crack. A centered fan must join two such regions of constant stress, and in the fan

$$\sigma_{rr} = \sigma_{\theta\theta} = \left(1 + \frac{3\pi}{2}\right)\tau_Y - 2\theta\tau_Y,$$
$$\sigma_{r\theta} = \tau_Y \qquad \text{(region C)} \qquad (13c)$$

This stress field is familiar in the limit analysis of double-edge notched thick plates [13]. It is emphasized that the boundary of the slip-line field in Fig. 5 is not intended to represent the elastic-plastic boundary.

Large strains can occur only when slip lines focus, as in the centered fans, but not in constant stress regions (A and B) unless strains are uniformly large along the straight slip lines and thus

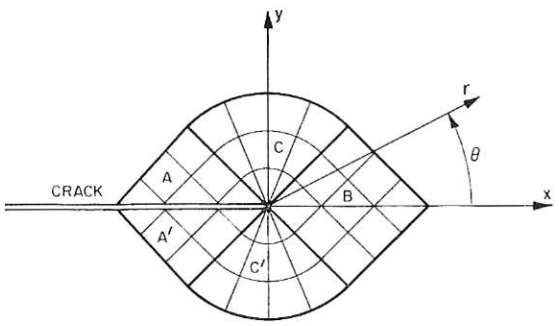

Fig. 5 Perfectly plastic plane-strain slip-line field at a crack tip; constant stress regions A and B joined by centered fan C

out toward the elastic-plastic boundary (where strains must be small). One then anticipates strains on the order of initial yield values in the constant stress regions. Only the strain singularity in the centered fan enters the results toward which we are heading. Assume elastic incompressibility for the moment, and that principal stress and strain directions coincide. Then $\epsilon_{rr} = \epsilon_{\theta\theta} = 0$ in the fan and displacements are thus representable in the form

$$u_r = f'(\theta), \qquad u_\theta = -f(\theta) + g(r),$$
$$\text{where } g(0) = f(\pi/4) = 0 \qquad (14a)$$

These equations apply to velocities [12] rather than displacements in a proper incremental theory. The nonvanishing strain component in the fan is

$$\gamma_{r\theta} = \frac{1}{r}\frac{\partial u_r}{\partial\theta} + \frac{\partial u_\theta}{\partial r} - \frac{u_\theta}{r}$$
$$= \frac{1}{r}\left[f''(\theta) + f(\theta) + rg'(r) - g(r)\right] \qquad (14b)$$

Now consider the path independent integral J (which was discovered as an extension of work directed toward establishing the strength of the $\gamma_{r\theta}$ singularity in this problem). Taking Γ as a circle of radius r centered at the crack tip and employing polar components,

$$J = r\int_{-\pi}^{+\pi}\left\{W\cos\theta - \sigma_{rr}\left[\epsilon_{rr}\cos\theta - \left(\frac{1}{2}\gamma_{r\theta} - \omega\right)\sin\theta\right]\right.$$
$$\left. - \sigma_{r\theta}\left[\left(\frac{1}{2}\gamma_{r\theta} + \omega\right)\cos\theta - \epsilon_{\theta\theta}\sin\theta\right]\right\}d\theta \qquad (15)$$

Here ω is the rotation, measured positive contraclockwise. We evaluate the integral by letting $r \to 0$, so that only the portion of the integral over the centered fans contribute. The near tip stress state is given by equations (13). Limiting forms of strain, rotation, and energy density in the fan C are now given. Note that $g'(0)$ exists since it is proportional to the finite extensional strain resulting as the tip is approached along the positive x axis, and is thus the limit of $g(r)/r$. Thus

$$\gamma_{r\theta} \to \gamma_Y\frac{R(\theta)}{r} \qquad \text{as } r \to 0 \text{ in } C, \qquad (16a)$$

from equation (14b). Here $\gamma_Y = \tau_Y/G$ is the initial yield strain in shear, and the function $R(\theta)$ is defined so that

$$\gamma_Y R(\theta) \equiv f''(\theta) + f(\theta) \qquad (16b)$$

Note that if $g(r)$ was a linear function of r throughout the plastic zone instead of just near the tip and if the straight fan line extended to the elastic-plastic boundary, then (16a) would be an equality throughout the zone and $R(\theta)$ would be the distance to the elastic-plastic boundary along a ray at angle θ. Thus we interpret $R(\theta)$ as an approximate indication of the extent of the plastically strained region. The rotation ω may be shown to approach $-\gamma_{r\theta}/2$ as $r \to 0$. The energy density appropriate to an incompressible nonhardening material is

$$W = \int\tau(\gamma)d\gamma = \begin{cases}\frac{1}{2}G\gamma^2 & \text{if } \gamma < \gamma_Y \\ \tau_Y\gamma - \frac{1}{2}G\gamma_Y^2 & \text{if } \gamma > \gamma_Y\end{cases} \qquad (17a)$$

where γ is the principal resolved in-plane shear strain. Thus

$$W \to \tau_Y\gamma_Y\frac{R(\theta)}{r} \qquad \text{as } r \to 0 \text{ in } C. \qquad (17b)$$

While it was simplest to perform calculations for an incompressible material, one may show that the asymptotic form for $\gamma_{r\theta}$ in equation (16a) as well as all subsequent formulas in this section apply also to an elastically compressible material.

The average value of $R(\theta)$ is now determined in terms of J by letting $r \to 0$ in equation (15), resulting in

$$J = 2\tau_Y\gamma_Y \int_{\pi/4}^{3\pi/4} R(\theta)\left[\cos\theta + \left(1 + \frac{3\pi}{2} - 2\theta\right)\sin\theta\right] d\theta. \tag{18}$$

Another useful form results by solving for displacements as $r \to 0$ in the fan. Converting equations (14a) to Cartesian components and employing equation (16b), one finds

$$u_y \to \gamma_Y \int_{\pi/4}^{\theta} R(\theta)\sin\theta d\theta, \qquad u_x \to \gamma_Y \int_{\pi/4}^{\theta} R(\theta)\cos\theta d\theta \quad \text{as } r \to 0 \text{ in } C. \tag{19a}$$

An integration by parts in equation (18) then leads to

$$J = 2\tau_Y \int_{\pi/4}^{3\pi/4} u_y(\theta)(3 + \operatorname{ctn}^2\theta)d\theta \tag{19b}$$

where $u_y(\theta)$ is the near tip vertical displacement in the fan.

Plastic Zone Extent and Crack Opening Displacement. We define the "crack opening displacement" δ_t as the total separation distance between upper and lower crack surfaces at the tip due to the strain singularity of the fan:

$$\delta_t = 2u_y(3\pi/4). \tag{20}$$

A lower bound on δ_t is established from equation (19b) since $u_y(\theta)$ is monotonic by equation (19a):

$$J < \tau_Y\delta_t \int_{\pi/4}^{3\pi/4} (3 + \operatorname{ctn}^2\theta)d\theta$$

$$\therefore \delta_t > \frac{J}{(2+\pi)\tau_Y}\left(= \frac{\pi(1-\nu^2)\sigma_\infty^2 a}{(2+\pi)\tau_Y E}, \text{ small-scale yielding}\right) \tag{21}$$

The latter form employs the small-scale yielding relation between J and the stress-intensity factor appropriate to the crack of length $2a$ in a remotely uniform stress field. A similar bound is obtained for the maximum value $R_{\max}$ of the function $R(\theta)$, and thus approximately for the maximum extent of the yielded region. From equation (18),

$$J \leqslant 2\tau_Y\gamma_Y R_{\max} \int_{\pi/4}^{3\pi/4} \left[\cos\theta + \left(1 + \frac{3\pi}{2} - 2\theta\right)\sin\theta\right] d\theta$$

$$\therefore R_{\max} \geqslant \frac{J}{\sqrt{2}(2+\pi)\tau_Y\gamma_Y}\left(= \frac{2\pi(1-\nu)}{\sqrt{2}(2+\pi)}\left(\frac{\sigma_\infty}{2\tau_Y}\right)^2 a, \text{ small-scale yielding}\right) \tag{22}$$

The path integral leads to no upper bounds on deformation measures, but rough approximations can be obtained by choosing a reasonable form for the functions $R(\theta)$ or $u_y(\theta)$, containing an unknown constant, and employing the J integral to determine the constant. Experience with nonhardening solutions in the antiplane strain case [14] suggest that, while $R(\theta)$ and $u_y(\theta)$ will have a unique dependence on θ in the small-scale yielding range, the θ dependence will vary considerably with applied stress level and detailed specimen shape in the large-scale yielding range. Thus no simple approximation will be uniformly valid, and we here choose approximations appropriate to a small plastic region confined to the vicinity of the crack tip. Anticipating that the plastic region will then be approximately symmetrical about the midline of the fan, $\theta = \pi/2$, from equations (19a) and (20) we will have $u_y(\theta) \approx \delta_t/4$ plus a function of θ that is antisymmetric about $\theta = \pi/2$. This antisymmetric term contributes nothing to the integral in equation (19b), and

$$J \approx \frac{1}{2}\tau_Y\delta_t \int_{\pi/4}^{3\pi/4} (3 + \operatorname{ctn}^2\theta)d\theta$$

$$\therefore \delta_t \approx \frac{2J}{(2+\pi)\tau_Y} = \frac{2\pi(1-\nu^2)\sigma_\infty^2 a}{(2+\pi)\tau_Y E}, \text{ small-scale yielding.} \tag{23}$$

Were a slip-line construction similar to Fig. 5 made in the antiplane strain case, a centered fan of shear lines would result ahead of the crack for $|\theta| < \pi/2$, while constant stress regions of parallel shear lines would result above and below the crack line. Exact solutions [14] lead to an elastic-plastic boundary cutting into the crack along the boundaries of the fan. Thus one might assume a form for $R(\theta)$ cutting into the crack tip along the fan boundaries in Fig. 5. Choosing such a form symmetric about $\pi/2$,

$$R(\theta) \approx R_{\max}\cos[2(\theta - \pi/2)], \tag{24a}$$

and equation (18) leads to

$$J \approx 2\tau_Y\gamma_Y R_{\max} \int_{\pi/4}^{3\pi/4} \cos(2\theta - \pi) \times \left[\cos\theta + \left(1 + \frac{3\pi}{2} - 2\theta\right)\sin\theta\right] d\theta$$

$$\therefore R_{\max} \approx \frac{3J}{2\sqrt{2}(2+\pi)\tau_Y\gamma_Y} = \frac{3\pi(1-\nu)}{\sqrt{2}(2+\pi)}\left(\frac{\sigma_\infty}{2\tau_Y}\right)^2 a, \quad \text{(small-scale yielding).} \tag{24b}$$

The approximations made here are quite arbitrary and our method includes no scheme for assessing errors. Other seemingly "reasonable" choices for functional forms could shift the approximations either way within constraints set by the lower bounds.

Blunting of the Crack Tip. Having just seen an analysis predicting no large strain concentration directly ahead of the tip of a sharp crack, one might wonder how cracks can propagate in materials for which the hydrostatic stress elevation alone is insufficient to cause fracture. Fig. 6 suggests an answer. The crack tip is progressively blunting under increasing load, and a slip-line pattern very different from that in Fig. 5 results over a small region comparable in size to the opening displacement δ_t. The fans C and C' become noncentered, and their straight slip lines focus intense deformation into a region D directly ahead of the tip. The progressively blunting tip has been drawn as a semicircle in Fig. 6 for simplicity of illustration, and the associated exponential spiral slip-line field [12] extends a distance 1.9 δ_t ahead of the tip. From the foregoing approximations, $\delta_t \approx 2\gamma_Y R_{\max}$, so that the intense deformation region is extremely small and Fig. 6 is essentially Fig. 5 magnified in linear dimensions by a large factor of order one over the initial yield strain. Since the blunted region is small, an effective procedure would be to perform an incremental analysis by regarding the displacement rate perpendicular to the boundary of region D as given by the rate of increase in the function $u_r(\theta)$, equation (14a), with θ now interpreted as the inclination angle of noncentered fan lines with the x-axis. The motivation is that, far from the blunted region, this angle will coincide with the polar angle θ, and it is known [12] that straight fan lines transmit a spatially constant displacement rate parallel to themselves. While such an analysis has not yet been carried out for contained plasticity, a similar analysis for a fully plastic problem has been carried out by Wang [15].

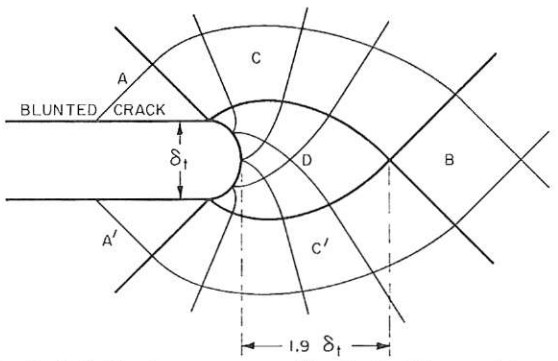

Fig. 6 Crack tip blunting creates a small region D of intense deformation ahead of the crack. This is Fig. 5 magnified in linear dimensions by a large factor of the order of one over the initial yield strain.

Barenblatt-Dugdale Crack Model

Sharp cracks lead to strain singularities. The Griffith theory [16] of elastic brittle fracture ignores this perhaps unrealistic prediction of conditions at the tip, and employs an energy balance to set the potential energy decrease rate due to crack extension equal to the energy of the newly created crack surfaces. An alternate approach due to Barenblatt [17] removes the singularity by considering a cohesive zone ahead of the crack, postulating that the influence of atomic or molecular attractions is representable as a restraining stress acting on the separating surfaces, Fig. 7(*a*). The restraining stress $\sigma(\delta)$ may be viewed as a function of separation distance δ as in Fig. 7(*b*). Although mathematical difficulties apparently prohibited Barenblatt from detailed solutions for specific restraining stress functions, we here take the view that a σ versus δ curve falling off to zero is given so that a fracture criterion requires no special assumptions not inherent to the model. A mathematically similar but conceptually different model was proposed by Dugdale [18] to discuss plane-stress yielding in sheets. There the influence of yielding was represented approximately by envisioning a longer crack extending into the region with yield level stresses opposing its opening. For reasons that are not yet clear, some metals actually reveal a narrow slitlike plastic zone [19] ahead of the crack of height approximately equal to sheet thickness when the zone is long compared to the thickness dimension. Except for a perturbation near the tip, yielding then consists of slip on 45-deg planes through the thickness so that plastic strain is essentially the separation distance divided by the thickness. Restraining stresses typical of plane-stress yielding are shown in Fig. 7(*b*).

We may evaluate our integral J by employing path independence to shrink the contour Γ down to the lower and upper surfaces of the cohesive zone as in Fig. (7)*a*. Then, since $dy = 0$ on Γ,

$$J = -\int_\Gamma \mathsf{T}\cdot\frac{\partial \mathbf{u}}{\partial x}\,ds$$

$$= -\int_{\text{cohes zone}} \sigma(\delta)\,\frac{d\delta}{dx}\,dx$$

$$= -\int_{\text{cohes zone}} \frac{d}{dx}\left\{\int_0^\delta \sigma(\delta)d\delta\right\}dx$$

$$= \int_0^{\delta_t} \sigma(\delta)d\delta \tag{25}$$

where δ_t is the separation distance at the crack tip. Thus, if the crack configuration is one of many for which J is known, we are able to solve for the crack opening displacement directly from the force-displacement curve.

Equivalence of Griffith and Cohesive Force Theories. Now let us compare to Griffith theory of elastic brittle fracture with the fracture prediction from the Barenblatt-type cohesive force model. Letting δ^* be the separation distance in Fig. 7(*b*) when the atoms at the crack tip can be considered pulled out of range of their neighbors, the value of J which will just cause crack extension (or, if crack extension is considered as reversible, will maintain equilibrium at the current crack length) is then

$$J = \int_0^{\delta^*} \sigma(\delta)d\delta \qquad \text{(Cohesive theory)} \tag{26a}$$

On the other hand, the Griffith theory regards the total potential energy of a cracked body as $P + 2Sl$, where l is crack length, S is surface energy, and P is the potential energy defined by the continuum mechanics solution without regard to cohesive forces. Determining equilibrium by setting the variation in total potential to zero,

$$-\frac{\partial P}{\partial l} = 2S \qquad \text{(Griffith theory)} \tag{26b}$$

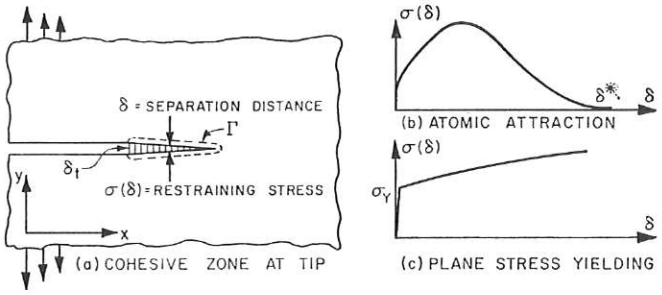

Fig. 7 Dugdale-Barenblatt crack model. (*a*) Cohesive zone at crack tip with restraining stress dependent on separation distance; (*b*) force-displacement relation for atomic attraction in elastic brittle fracture; (*c*) for plane-stress plastic yielding in thin sheet.

We conclude that the Griffith theory is identical to a theory of fracture based on atomic cohesive forces, regardless of the force-attraction law, so long as the usual condition is fulfilled that the cohesive zone be negligible in size compared to characteristic dimensions (small-scale yielding). This is because the area under the force-separation curve is by definition twice the surface energy and, as we have noted, for small-scale yielding J is equal to the potential energy decrease rate as calculated from the usual continuum solution.

This simple demonstration explains the close correspondence found by Goodier and Kanninen [20] between a Griffith theory and numerical calculations for specific nonlinear force attraction laws. Indeed, the discrepancies must be due to the peculiarities of their modeling the discrete atomic structure along the separating plane. Willis [21] has recently demonstrated the identity of the two theories through a detailed calculation based on complex variable methods in plane elasticity. His work includes a discussion of problems in interpreting the model and an extension to the constant velocity crack problem.

Dugdale Model for Plane-Stress Yielding. Strain-hardening behavior is readily included in the Dugdale model; analyses to date have been limited to perfect plasticity. For example, with linear work-hardening

$$\sigma(\delta) = \sigma_Y + E_w\frac{\delta}{h} \tag{27a}$$

where h is sheet thickness, E_w a tangent modulus, and the strain approximated by δ/h, equation (23) gives the crack opening displacement as

$$\delta_t = \frac{\sigma_Y h}{E_w}\left\{\left(1 + \frac{2E_w J}{h\sigma_Y{}^2}\right)^{1/2} - 1\right\}$$

$$\left(= \frac{\sigma_Y h}{E_w}\left\{\left[1 + 2\pi\frac{E_w}{E}\left(\frac{\sigma_\infty}{\sigma_Y}\right)^2\frac{a}{h}\right]^{1/2} - 1\right\},\right.$$

$$\left.\text{small-scale yielding}\right) \tag{27b}$$

In the latter form the plane-stress value of J for the crack length $2a$, appropriate for small-scale yielding, has been used. With negligible strain-hardening ($E_w = 0$) this becomes

$$\delta_t = \frac{J}{\sigma_Y}\left(= \frac{\pi\sigma_\infty{}^2 a}{E\sigma_Y},\ \text{small-scale yielding}\right) \tag{27c}$$

as is obvious from equation (25). Other stress-separation distance functions are readily handled. In particular, a function first rising and then falling to zero might be useful for studying fracture by necking to zero thickness in ductile foils.

The complete solution of the nonhardening Dugdale model for the configuration in Fig. 4 leads to [4]

$$\delta_t = \frac{8\sigma_Y a}{\pi E}\log\left[\sec\left(\frac{\pi\sigma_\infty}{2\sigma_Y}\right)\right] = \frac{\pi\sigma_\infty{}^2 a}{E\sigma_Y} + \dots$$

$$R_{\max} = a\left[\sec\left(\frac{\pi\sigma_\infty}{2\sigma_Y}\right) - 1\right] = \frac{\pi^2}{8}\left(\frac{\sigma_\infty}{\sigma_Y}\right)^2 a + \dots \tag{28}$$

for the opening displacement and length of the plastic zone. A Taylor development of the first of these checks equation (27c) at low applied stress levels. Further, since $J = \sigma_Y \delta_t$ we may use this model to estimate the deviation of J from its linear elastic value in the large-scale yielding range. Taking the results for δ_t and $R_{\max}$ as representative of plane stress, as observations suggest [18, 19] for materials in which Dugdale zones actually form, we may compare small-scale yielding behavior in plane stress with plane strain as approximated by equations (23) and (24b). Thus, for $\nu = 0.3$, one finds a plane-strain opening displacement which is 61 percent of the plane-stress value for a Mises material ($\sigma_Y = \sqrt{3}\tau_Y$) and 70 percent for a Tresca material ($\sigma_Y = 2\tau_Y$). The plane-strain value of $R_{\max}$ is 55 percent the plane-stress value for a Mises material and 73 percent for a Tresca material. Any compensation for stress biaxiality in raising the Dugdale yield stress in a Mises material above the uniaxial yield would tend to reduce the differences between the Mises and Tresca comparisons. Etching observations [22] suggest a plane-strain to plane-stress zone size ratio in the neighborhood of one half.

Strain Concentration at Smooth-Ended Notch Tips

Consider a flat-surfaced notch with a smooth tip. Letting ϕ the tangent angle at a point on the tip, as in Fig. 8, and $r_t(\phi)$ the radius of curvature, equation (4) becomes

$$J = \int_{\Gamma_t} W dy = \int_{-\pi/2}^{+\pi/2} W[\epsilon(\phi)] r_t(\phi) \cos\phi d\phi \qquad (29)$$

Here $\epsilon(\phi)$ is the surface extensional strain at the point with tangent angle ϕ, and estimates of the maximum strain will require an approximate choice for the functional dependence on ϕ. A lower bound is immediate since $W[\epsilon(\phi)] \leqslant W(\epsilon_{\max})$:

$$J \leqslant W(\epsilon_{\max}) \int_{\Gamma_t} dy = 2hW(\epsilon_{\max}), \qquad (30)$$

where $2h$ is the distance between the flat notch surfaces. For a linear elastic material

$$W = \frac{1}{2}\sigma\epsilon = \frac{E\epsilon^2}{2(1-\nu^2)} \text{ for plane strain}$$

$$= \frac{E\epsilon^2}{2} \text{ for plane stress.} \qquad (31)$$

Now consider a notch in the configuration in Fig. 4, which is sufficiently narrow so that the sharp crack value of J is appropriate. Then for either plane stress or plane strain one has for the maximum concentrated stress

$$\sigma_{\max} \gtrsim \sqrt{\pi}\sigma_\infty \sqrt{a/h} = 1.77\sigma_\infty\sqrt{a/h}, \qquad (32)$$

regardless of the detailed shape of the curved notch tip. An interesting unsolved problem is the determination of the optimum proportioning of a notch tip. The lower bound would actually be obtained if the surface stress were constant at every point on the curved tip, and the problem is to determine the shape of a tip leading to constant stress (if such a shape exists).

For approximations to the strain concentration through equation (29), we recall a feature of the linear elastic problem of an ellipsoidal inclusion in an infinite matrix subjected to a uniform remote stress state. All strain components are spatially constant within the inclusion [23]. The same result applies to an ellipsoidal void, in that surface displacements are compatible with the homogeneous deformation of an imagined inclusion having zero elastic moduli. Thus, for an elliptical hole in a linear elastic plate, loaded symmetrically so as to cause no shear or rotation of the imagined inclusion, surface strains are given through the usual tensor transformation as

$$\epsilon(\phi) = \epsilon_{\max}\cos^2\phi + \epsilon_{\min}\sin^2\phi. \qquad (33a)$$

Here the ϕ notation is as in Fig. 8, $\epsilon_{\max}$ is the extensional strain at the semimajor axis ($\phi = 0, \pi$), and $\epsilon_{\min}$ at the semiminor axis ($\phi = \pi/2, 3\pi/2$). Thus, presuming this same interpretation of the surface strains to be approximately valid in other cases and that $\epsilon_{\min}$ is small compared to $\epsilon_{\max}$,

$$J \approx \int_{-\pi/2}^{+\pi/2} W(\epsilon_{\max}\cos^2\phi) r(\phi)\cos\phi d\phi \qquad (33b)$$

For linear elastic behavior and the narrow notch in Fig. 4 with a semicircular tip, $r_t(\phi) = r_t$ (a const), this leads to

$$\sigma_{\max} \approx \sqrt{\frac{15\pi}{8}}\sigma_\infty\sqrt{a/r_t} = 2.43\sigma_\infty\sqrt{a/r_t} \qquad (34)$$

One would expect a higher number than the 2 factor for the narrow ellipse, although the 20 percent difference seems rather high. Presuming the material to behave in a perfectly plastic fashion once a yield stress σ_Y is attained on the notch surface, the energy density under plane-strain conditions is

$$W = \sigma_Y\epsilon - \frac{1}{2}\sigma_Y\epsilon_Y \qquad \text{for } \epsilon > \epsilon_Y = (1-\nu^2)\sigma_Y/E. \qquad (35a)$$

By equation (33b),

$$\left(\frac{\epsilon_{\max}}{\epsilon_Y}\right)^2 - \left(\frac{\epsilon_Y}{\epsilon_{\max}}\right)^{1/2}\left(\frac{\epsilon_{\max}}{\epsilon_Y} - 1\right)^{5/2} \approx \frac{15J}{8\sigma_Y\epsilon_Y r_t} \qquad (35b)$$

whenever the maximum strain thus computed exceeds the initial yield ϵ_Y. The left side may be developed in a series and if we neglect all terms which approach zero when $\epsilon_{\max}/\epsilon_Y$ becomes large,

$$\epsilon_{\max} \approx \frac{3}{4}\left(\epsilon_Y + \frac{J}{\sigma_Y r_t}\right) \left(= \frac{3}{4}\epsilon_Y\left[1 + \pi\left(\frac{\sigma_\infty}{\sigma_Y}\right)^2\frac{a}{r_t}\right], \text{ small-scale yielding}\right) \qquad (35c)$$

This result differs negligibly from equation (35b) when $\epsilon_{\max}$ is greater than $3\epsilon_Y$. The lower bound of equation (30) leads to a formula identical to equation (35c), except that the factor $^3/_4$ is replaced by $^1/_2$. A power law relation $\sigma = \sigma_Y(\epsilon/\epsilon_Y)^N$ between surface stress and strain beyond the elastic limit leads to

$$\epsilon_{\max} \approx \epsilon_Y\left[\frac{(N+1/2)(N+3/2)\Gamma(N+1/2)}{\Gamma(1/2)\Gamma(N+1)}\frac{J}{\sigma_Y\epsilon_Y r_t}\right]^{1/(1+N)}. \qquad (36)$$

Here $\Gamma(\ldots)$ is the gamma function and terms of order ϵ_Y have been omitted for convenience in calculation.

As noted earlier, the approximations made are more or less arbitrary, and no guide is available for improving results. Results in this section are somewhat reminiscent of Neuber's discovery [24] that the product of maximum concentrated stress and strain are independent of the plastic region stress-strain relation for antiplane deformation. The author [4] later pointed out that this result is limited to small-scale yielding, and applies only to notches generated by stress trajectories of the sharp crack solution (and thus to a different notch shape for each different material). Since J is independent of the plastic region stress-strain relation for small-scale yielding, our present results show that the averaged energy density then does not depend on the particular stress-strain relation.

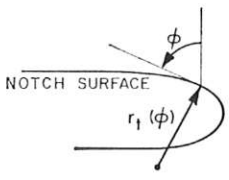

Fig. 8 Coordinates employed in description of notch surface; ϕ is tangent angle and $r_t(\phi)$ is radius of curvature

Acknowledgment

Support of this research by the Advanced Research Projects Agency, under Contract SD-86 with Brown University, is gratefully acknowledged.

References

1 Phillips, H. B., *Vector Analysis*, Wiley, 1959.

2 Irwin, G. R., "Fracture Mechanics," *Structural Mechanics (Proceedings of First Naval Symposium,)* Pergamon Press, 1960.

3 Eshelby, J. D., "The Continuum Theory of Lattice Defects," *Solid State Physics*, Vol. 3, Academic Press, 1956.

4 Rice, J. R., "The Mechanics of Crack Tip Deformation and Extension by Fatigue," *Fatigue Crack Growth*, ASTM Spec. Tech. Publ. 415, 1967.

5 Williams, M. L., "On the Stress Distribution at the Base of a Stationary Crack," JOURNAL OF APPLIED MECHANICS, Vol. 24, No. 1, TRANS. ASME, Vol. 79, Mar. 1957, pp. 109–114.

6 Rice, J. R., "Mathematical Analysis in the Mechanics of Fracture," to appear in *Treatise on Fracture*, Vol. 2, ed., Liebowitz, H., Academic Press.

7 Sanders, J. L., "On the Griffith-Irwin Fracture Theory," JOURNAL OF APPLIED MECHANICS, Vol. 27, No. 2, TRANS. ASME, Vol. 82, Series E, June 1960, pp. 352–353.

8 Thomas, A. G., "Rupture of Rubber, II, The Strain Concentration at an Incision," *Journal of Polymer Science*, Vol. 18, 1955.

9 Rice, J. R., and Drucker, D. C., "Energy Changes in Stressed Bodies Due to Void and Crack Growth," *International Journal of Fracture Mechanics*, Vol. 3, No. 1, 1967.

10 Bowie, O. L., and Neal, D. M., "The Effective Crack Length of an Edge Notch in a Semi-Infinite Sheet Under Tension," to appear in *International Journal of Fracture Mechanics*.

11 Rice, J. R., "Stresses Due to a Sharp Notch in a Work-Hardening Elastic-Plastic Material Loaded by Longitudinal Shear," JOURNAL OF APPLIED MECHANICS, Vol. 34, No. 2, TRANS. ASME, Vol. 89, Series E, June 1967, pp. 287–298.

12 Hill, R., *The Mathematical Theory of Plasticity*, Clarendon Press, Oxford, 1950.

13 Lee, E. H., "Plastic Flow in a V-Notched Bar Pulled in Tension," JOURNAL OF APPLIED MECHANICS, Vol. 19, No. 3, TRANS. ASME, Vol. 74 Sept. 1952, pp. 331–336.

14 Rice, J. R., "Contained Plastic Deformation Near Cracks and Notches Under Longitudinal Shear," *International Journal of Fracture Mechanics*, Vol. 2, No. 2, 1966.

15 Wang, A. J., "Plastic Flow in a Deeply Notched Bar With a Semi-Circular Root," *Quarterly of Applied Mathematics*, Vol. 11, 1954.

16 Griffith, A. A., "The Phenomena of Rupture and Flow in Solids," *Philosophical Transactions of the Royal Society*, London, Series A, Vol. 221, 1921.

17 Barenblatt, G. I., "Mathematical Theory of Equilibrium Cracks in Brittle Fracture," *Advances in Applied Mechanics*, Vol. 7, Academic Press, 1962.

18 Dugdale, D., "Yielding of Steel Sheets Containing Slits," *Journal of the Mechanics and Physics of Solids*, Vol. 8, 1960.

19 Hahn, G. T., and Rosenfield, A. R., "Local Yielding and Extension of a Crack Under Plane Stress," *Acta Metallurgica*, Vol. 13, No. 3, 1965.

20 Goodier, J. N., and Kanninen, M. F., "Crack Propagation in a Continuum Model With Nonlinear Atomic Separation Laws," Stanford University, Division of Engineering Mechanics, Technical Report 165, July 1966.

21 Willis, J. R., "A Comparison of the Fracture Criteria of Griffith and Barenblatt," *Journal of the Mechanics and Physics of Solids*, Vol. 15, 1967.

22 Hahn, G. T., and Rosenfield, A. R., "Experimental Determination of Plastic Constraint Ahead of a Sharp Crack Under Plane Strain Conditions," Ship Structure Committee Report, SSC-180, Dec. 1966.

23 Eshelby, J. D., "The Determination of the Elastic Field of an Ellipsoidal Inclusion and Related Problems," *Proceedings of the Royal Society*, London, Series A, Vol. 241, 1957.

24 Neuber, H., "Theory of Stress Concentration for Shear-Strained Prismatical Bodies With Arbitrary Nonlinear Stress-Strain Laws," JOURNAL OF APPLIED MECHANICS, Vol. 28, No. 4, TRANS. ASME, Vol. 83, Series E, 1961, Dec. 1961, pp. 544–550.